

**Supplementary Information for:**  
**Interplay between hydrophobicity and basicity toward the catalytic activity of isorecticular organocatalyst MOFs**

Sedigheh Abedi, Alireza Azhdari Tehrani, Hosein Ghasempour and Ali Morsali,\*

Department of Chemistry, Faculty of Sciences, Tarbiat Modares University, P.O. Box 14115-175, Tehran, Iran

<b>Figure S1.</b> FT-IR spectra of the ligands, L1 and RL1	Page 3
<b>Figure S2.</b> FT-IR spectra of the ligands, L2 and RL2.	Page 4
<b>Figure S3.</b> Mass spectra of the ligands, L2 and RL2.	Page 5
<b>Figure S4.</b> Mass spectra of the ligands, L1 and RL1.	Page 6
<b>Figure S5 .</b> (a) <sup>1</sup> H-NMR spectra of L1 and L2, (b) <sup>1</sup> H-NMR spectra of RL1 and RL2	Page 7
<b>Figure S6.</b> Comparative FT-IR spectra of TMU-6(L1) synthesized with different method and the recycled one after the condensation reaction.	Page 8
<b>Figure S7.</b> Comparative FT-IR spectra of TMU-21(L2) synthesized with different method and the recycled one after the condensation reaction	Page 9
<b>Figure S8.</b> Comparative FT-IR spectra of TMU-6(RL1) and the recycled one after the condensation reaction.	Page 10
<b>Figure S9.</b> Comparative FT-IR spectra of TMU-21(RL2) synthesized and the recycled one after the condensation reaction.	Page 11
<b>Figure S10.</b> Thermogravimetric analysis of TMU-6(L1) (blue line) and TMU-21(L2) (red line)	Page 12
<b>Figure S11.</b> Thermogravimetric analysis of TMU-6(RL1) (blue line) and TMU-21(RL2) (red line)	Page 13
<b>Figure S12.</b> PXRD patterns of TMU-6(L1), TMU-6(RL1), TMU-21(L2) and TMU-21(RL2) revealed that these four MOFs are isorecticular framework.	Page 14
<b>Figure S13.</b> PXRD patterns of simulated, as-synthesized, mechano-synthesized, activated, after reaction and water stability of TMU-6(L1).	Page 15
<b>Figure S14.</b> PXRD patterns of simulated, as-synthesized, mechano-synthesized, activated, after reaction and water stability of TMU-21(L2).	Page 16

<b>Figure S15.</b> PXRD patterns of simulated, mechano-synthesized, after reaction and water stability of TMU-6(L1) and TMU-6(RL1).	Page 17
<b>Figure S16.</b> PXRD patterns of simulated, mechano-synthesized, after reaction and water stability of TMU-21(L2) and TMU-21(RL2).	Page 19
<b>Table S1.</b> Catalytic performance of TMU-6(L1), TMU-6(RL1), TMU-21(L2) and TMU-21(RL2), obtained by mechanochemical synthesis, within aldol condensation of malonitrile with 2-cyclohexen-1-one, 24h. <b>Identification of the product:</b> 2-(cyclohex-2-enylidene)malononitrile	Page 20
<b>Table S2.</b> Time in depended catalytic performance of TMU-6(L1), TMU-6(RL1), TMU-21(L2) and TMU-21(RL2), obtained by mechanochemical synthesis within aldol condensation of malonitrile with 2-cyclopenten-1-one. <b>Identification of the product:</b> 2-(cyclopent-2-enylidene)malononitrile	Page 21
<b>Table S3.</b> Time in depended catalytic performance of TMU-6(L1), TMU-6(RL1), TMU-21(L2) and TMU-21(RL2), obtained by mechanochemical synthesis, within aldol condensation of malonitrile with 4,4-dimethylcyclohexen-1-one. <b>Identification of the product:</b> 2-(cyclopent-2-enylidene)malononitrile	Page 22
<b>Figure S17.</b> The images of the catalysts in H <sub>2</sub> O solvents after addition of toluene (up), in H <sub>2</sub> O solvents after addition of dichloromethane (down) (a) TMU-21(L2), (b) TMU-21(RL2), (c) TMU-6(L1) and (d) TMU-6(RL1).	Page 23
<b>Figure S18.</b> Yield-versus-time profile of aldol-type condensation reaction of (a) 2-cyclopenten-1-one and (b) 4,4-dimethyl-2-cyclohexen-1-one catalyzed by four MOF structures in the reaction conditions indicated in Table 1 of the manuscript.	Page 24
<b>Figure S19</b> Comparison of the catalyst reactivity of various substrates in the presence of different basic MOFs.	Page 25
<b>Figure S20.</b> Reusability of TMU-6(RL1) (gray) and TMU-21(L2) (orange) in aldol-type condensation reaction of 2-cyclopenten-1-one and 4,4-dimethyl-2-cyclohexen-1-one, respectively. (Conditions: catalyst (10 mol%), malononitrile, MeOH, 60 °C, 24h).	Page 25

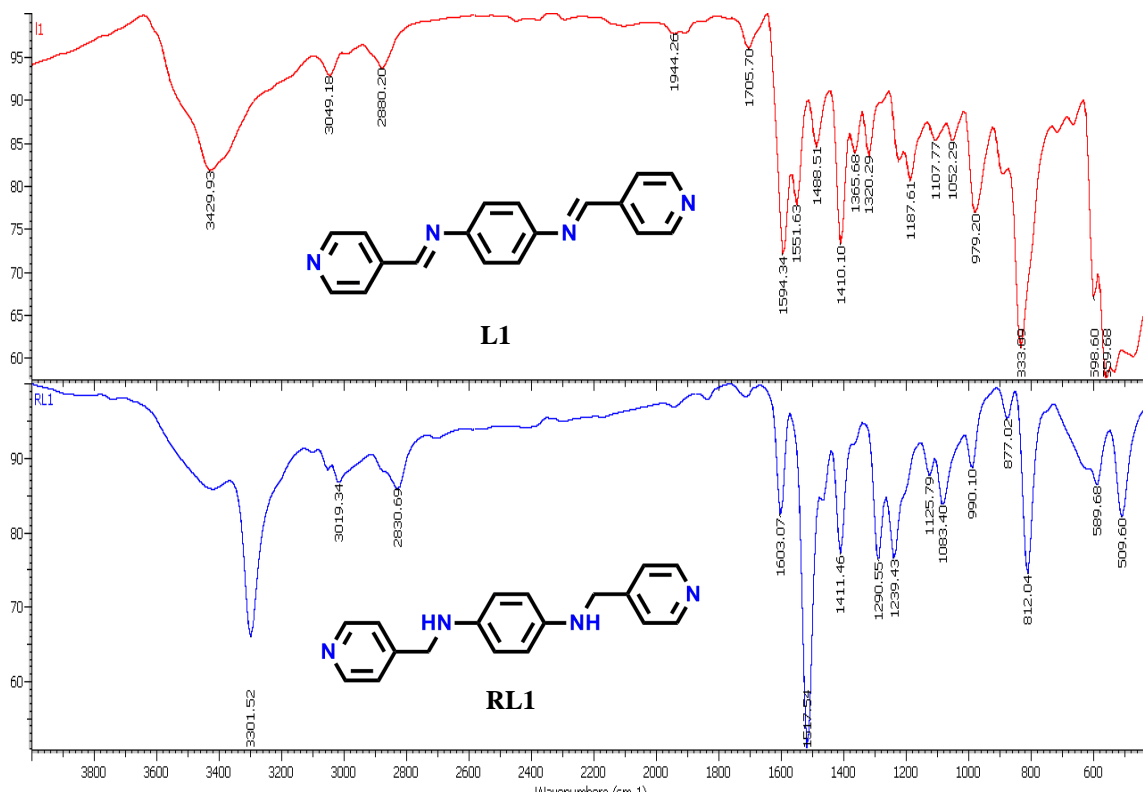


**Figure S1.** FT-IR spectra of the ligands, L1 and RL1.

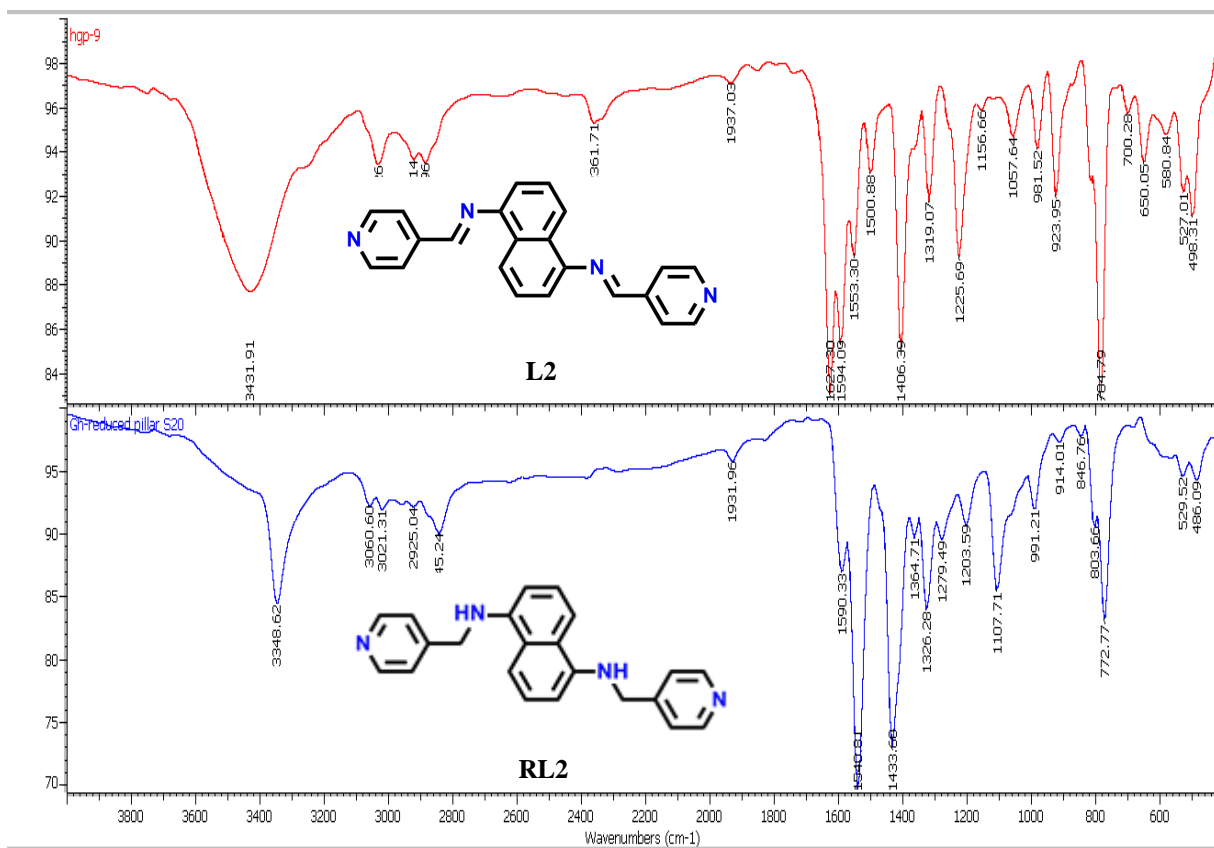


Figure S2. FT-IR spectra of the ligands, L2 and RL2.

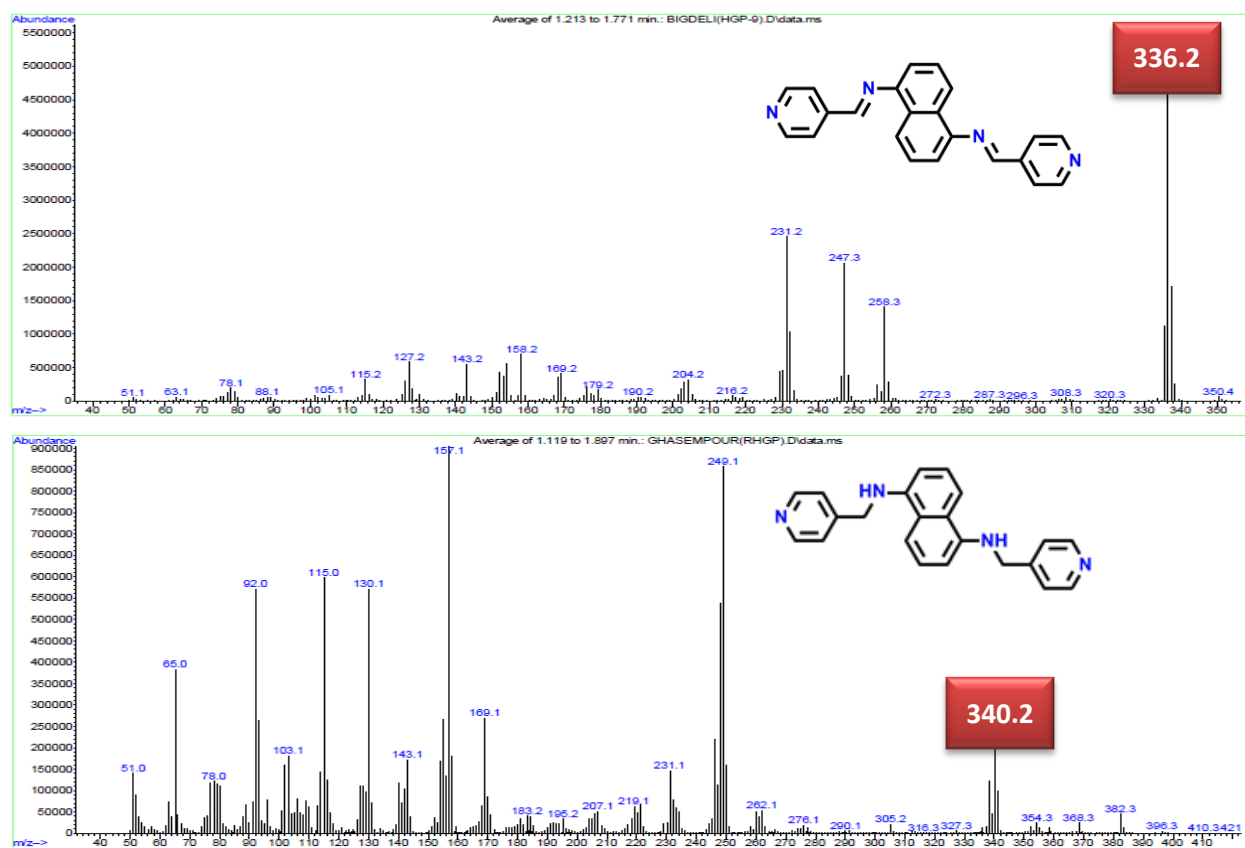
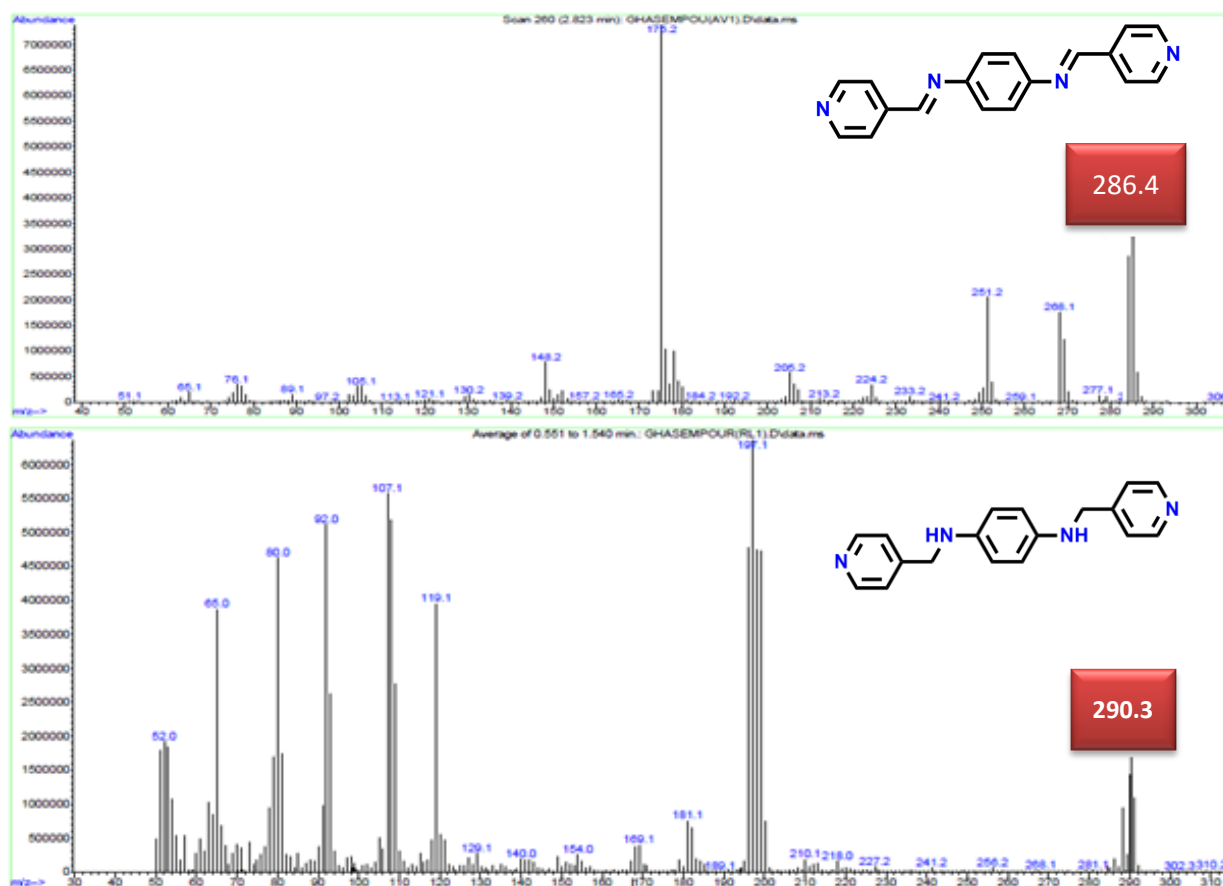


Figure S3. Mass spectra of the ligands, L2 and RL2.



**Figure S4.** Mass spectra of the ligands, L1 and RL1.

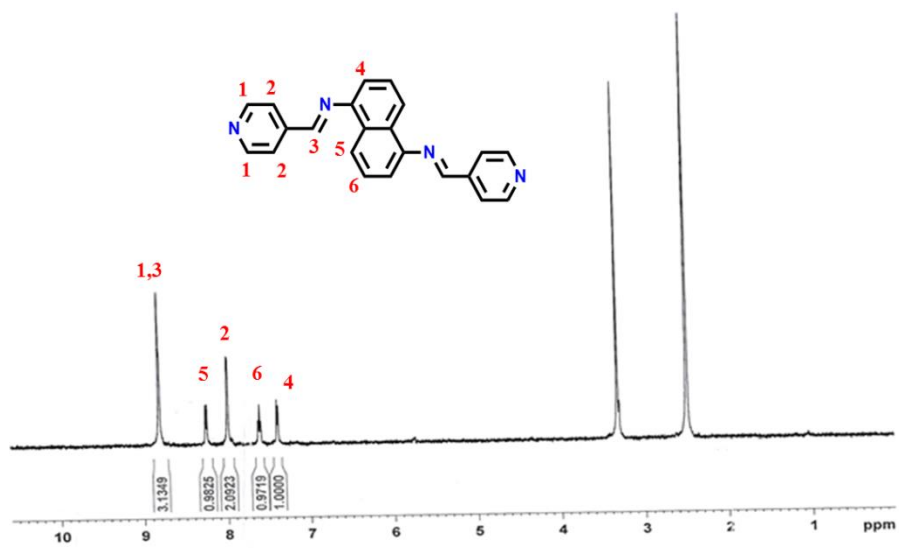
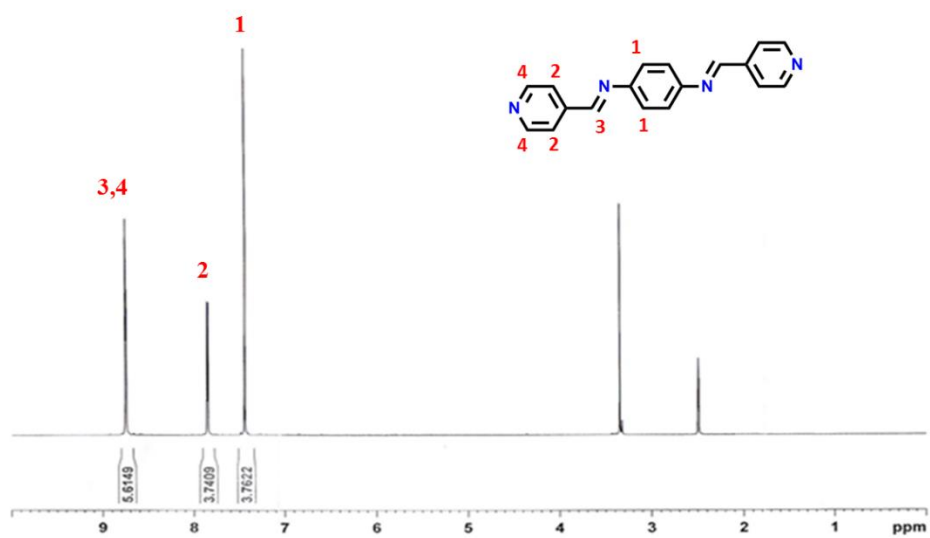


Figure S5 (a). <sup>1</sup>H-NMR spectra of L1 and L2

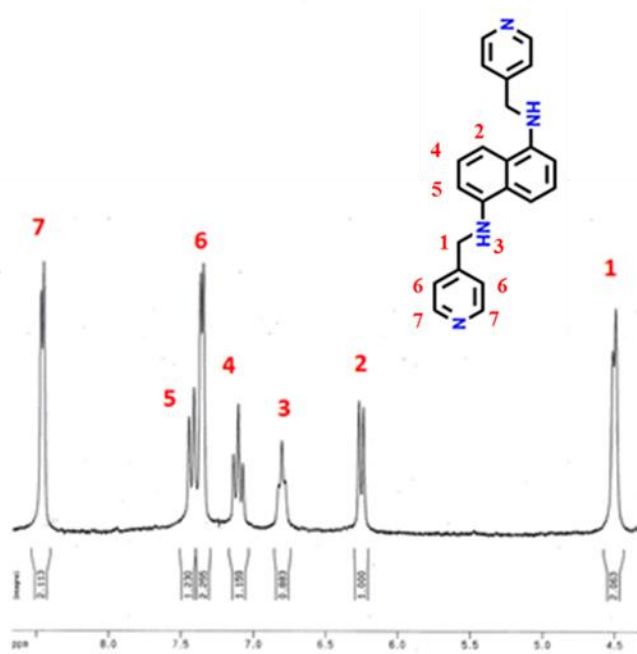
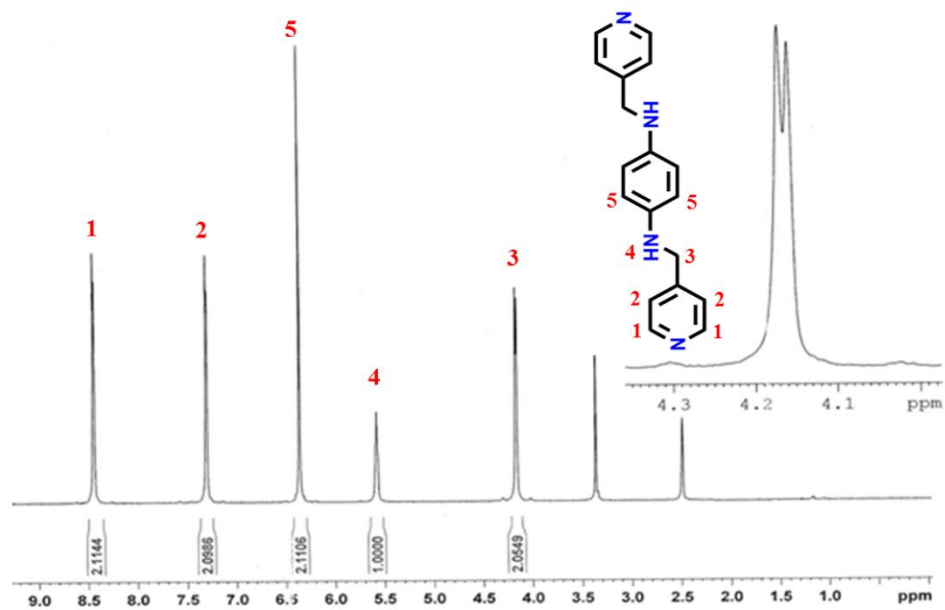
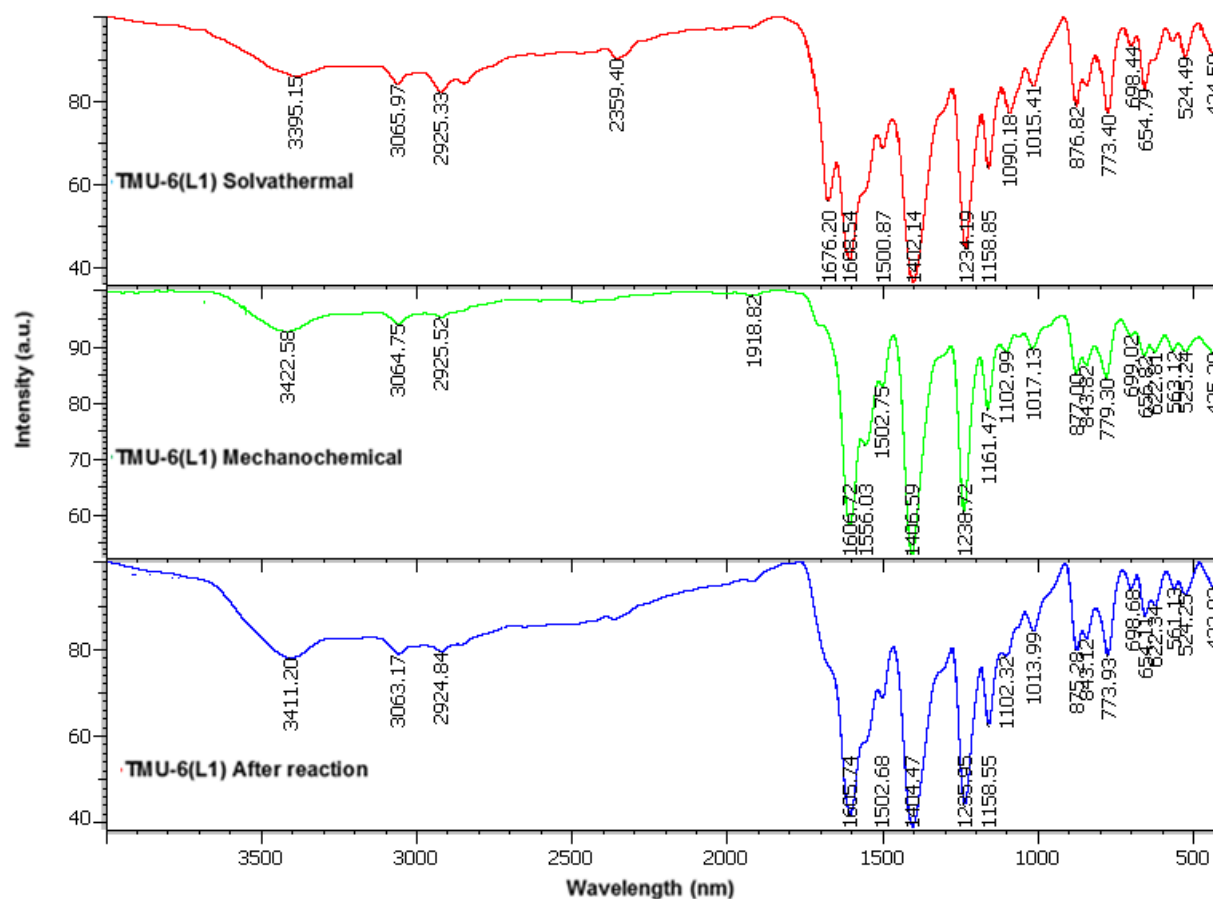


Figure S5 (b). <sup>1</sup>H-NMR spectra of RL1 and RL2.





**Figure S6.** Comparative FT-IR spectra of TMU-6(L1) synthesized with different method and the recycled one after the condensation reaction.

The FT-IR spectrum of the MOFs shows the same characteristic bands of the dicarboxylate groups of the H<sub>2</sub>oba ligands at ca. 1606 and 1404 cm<sup>-1</sup> for the asymmetric and symmetric vibrations, respectively, which indicate coordination of carboxylate ligands to metal ions. The absence of the expected characteristic bands at 1730–1690 cm<sup>-1</sup> for the protonated carboxylate groups indicates the complete deprotonation of H<sub>2</sub>oba ligand in the reaction with Zn ions. This point exists in FT-IR spectrum of all prepared MOFs.

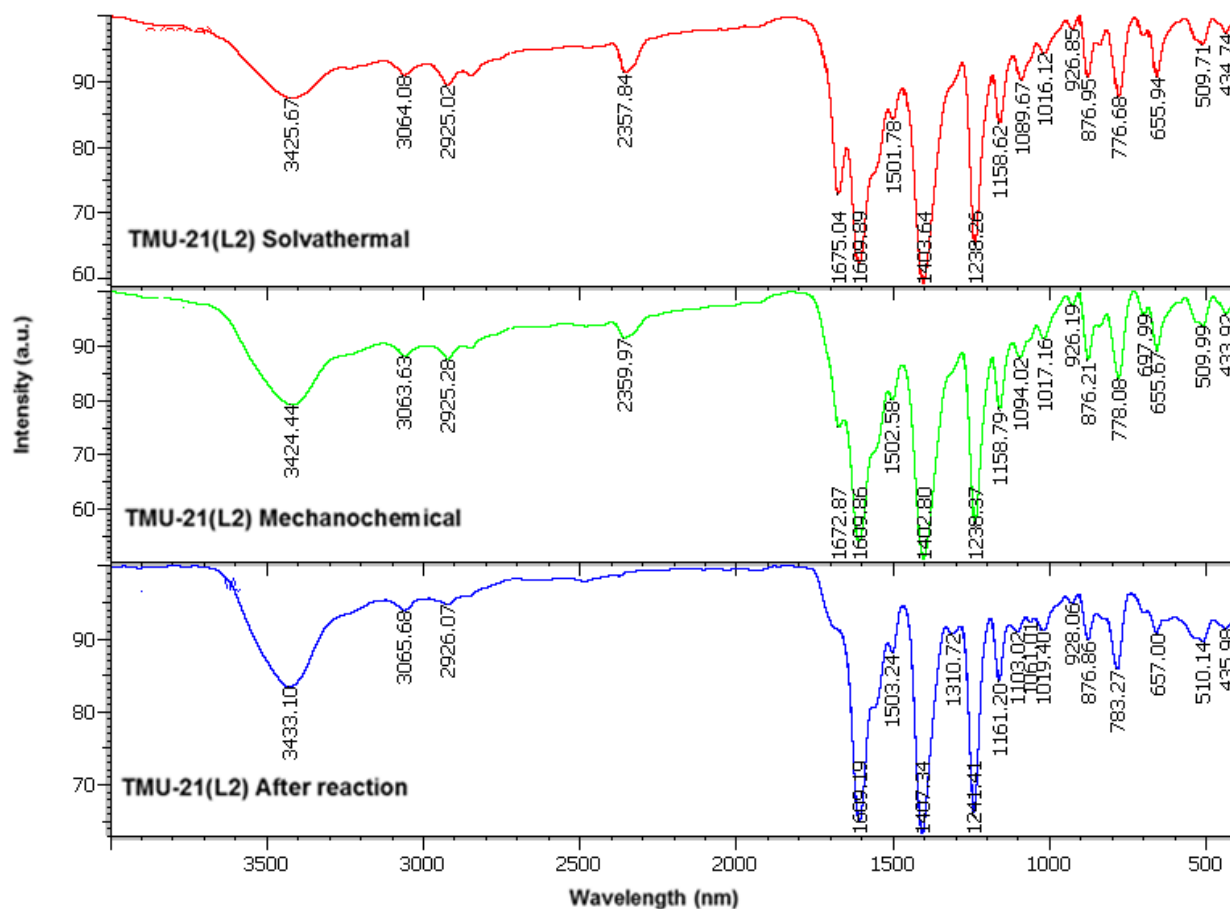


**Figure S7.** Comparative FT-IR spectra of TMU-21(L2) synthesized with different method and the recycled one after the condensation reaction.

The FT-IR spectrum of the MOFs shows the same characteristic bands of the dicarboxylate groups of the H<sub>2</sub>oba ligands at ca. 1609 and 1402 cm<sup>-1</sup> for the asymmetric and symmetric vibrations, respectively, which indicate coordination of carboxylate ligands to metal ions.

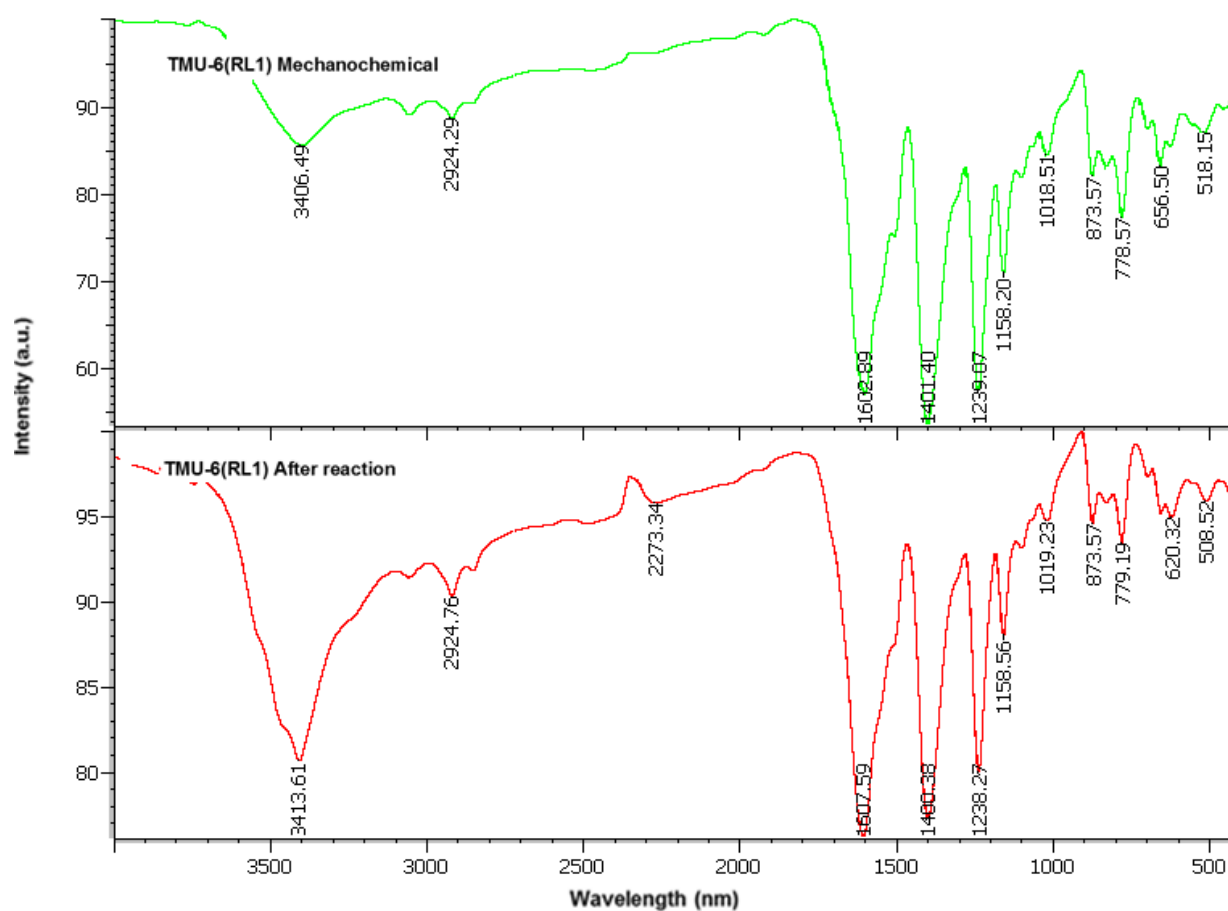


**Figure S8.** Comparative FT-IR spectra of TMU-6(RL1) and the recycled one after the condensation reaction.

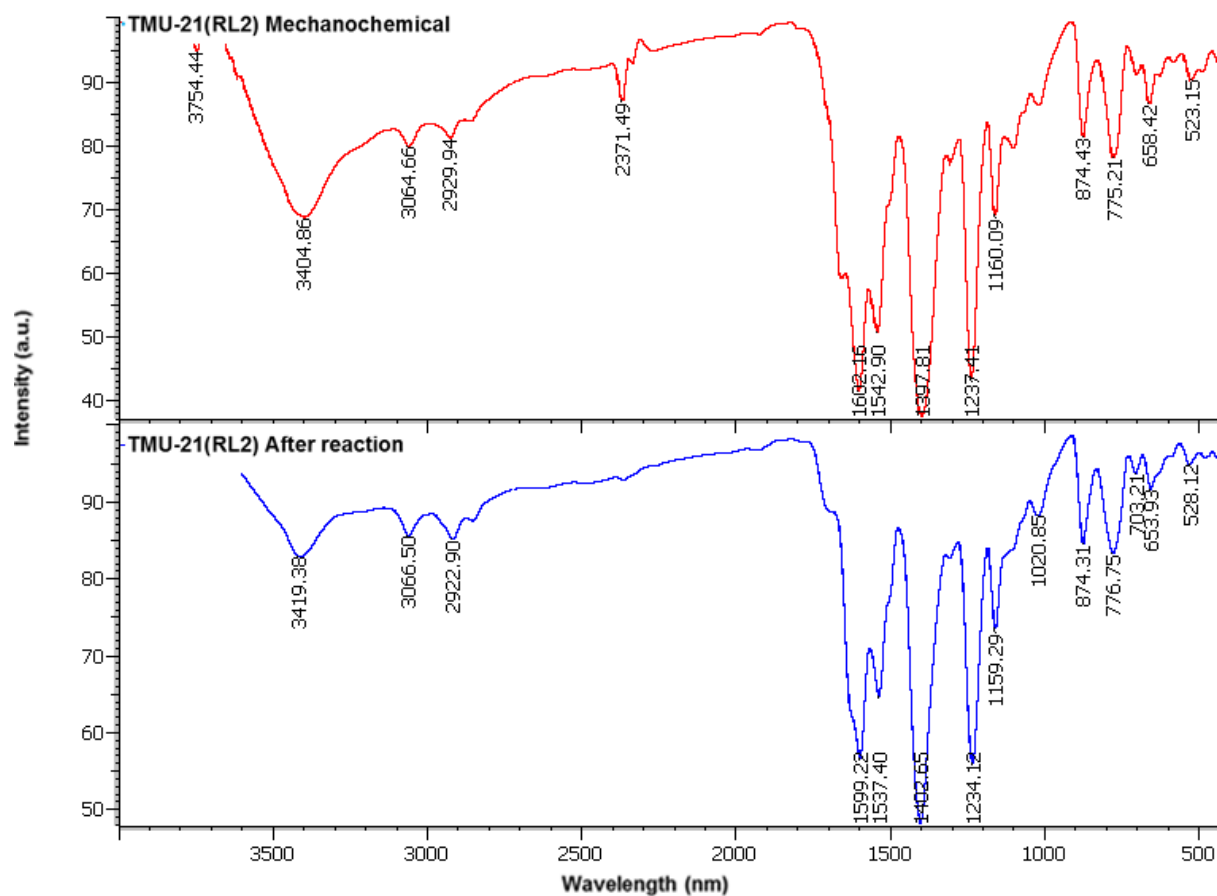


**Figure S9.** Comparative FT-IR spectra of TMU-21(RL2) synthesized and the recycled one after the condensation reaction.

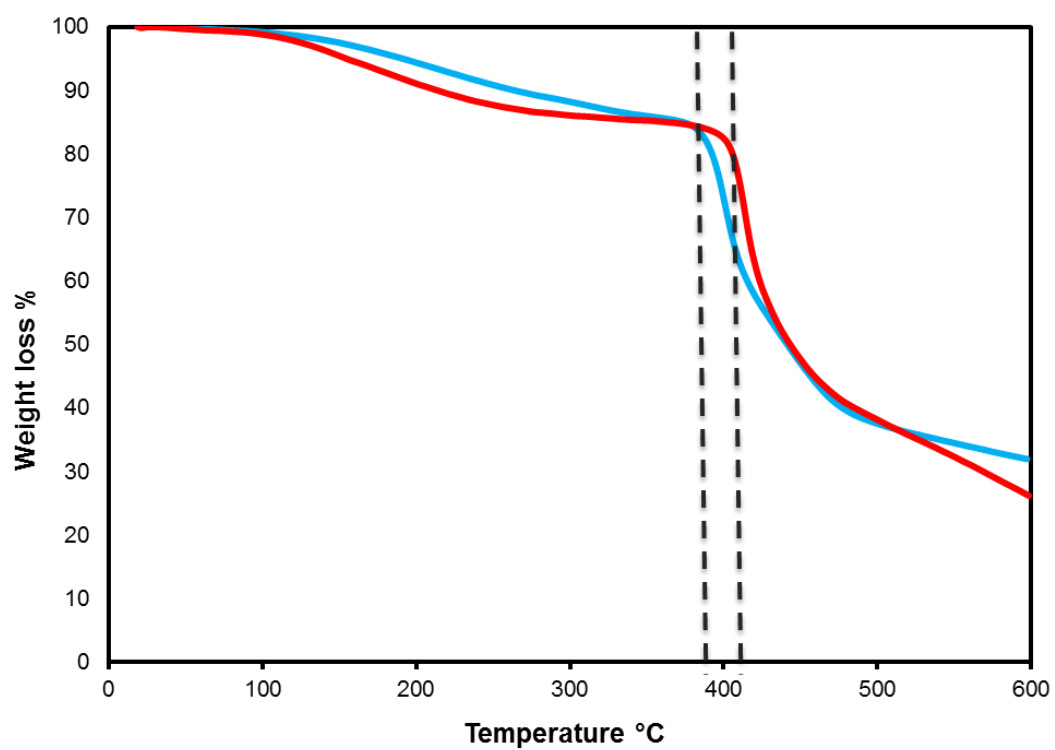


**Figure S10.** Thermogravimetric analysis of TMU-6(L1) (blue line) and TMU-21(L2) (red line)

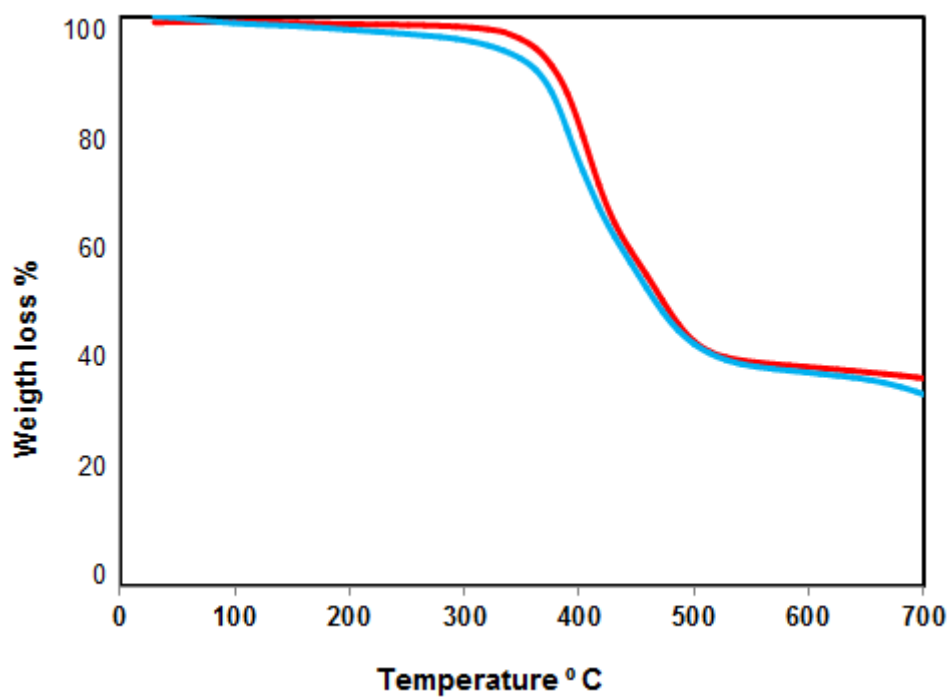


**Figure S11.** Thermogravimetric analysis of TMU-6(RL1) (blue line) and TMU-21(RL2) (red line)

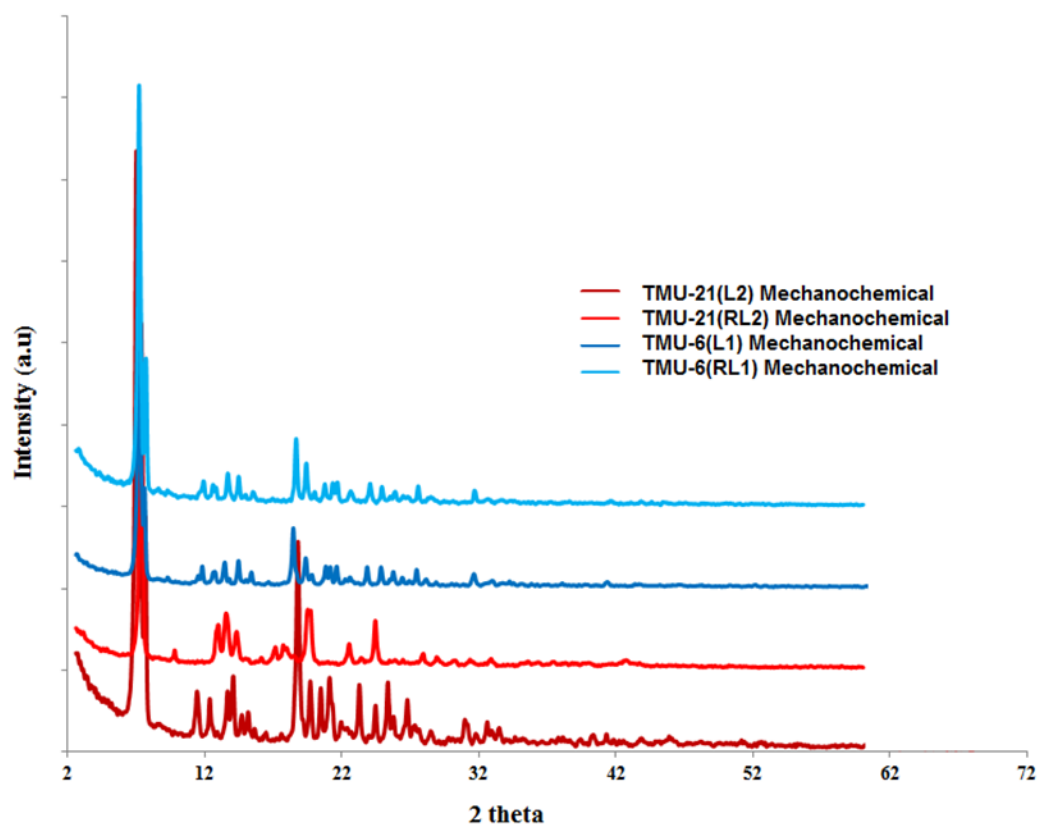


**Figure S12.** PXRD patterns of TMU-6(L1), TMU-6(RL1), TMU-21(L2) and TMU-21(RL2) revealed that these four MOFs are isorecticular framework.

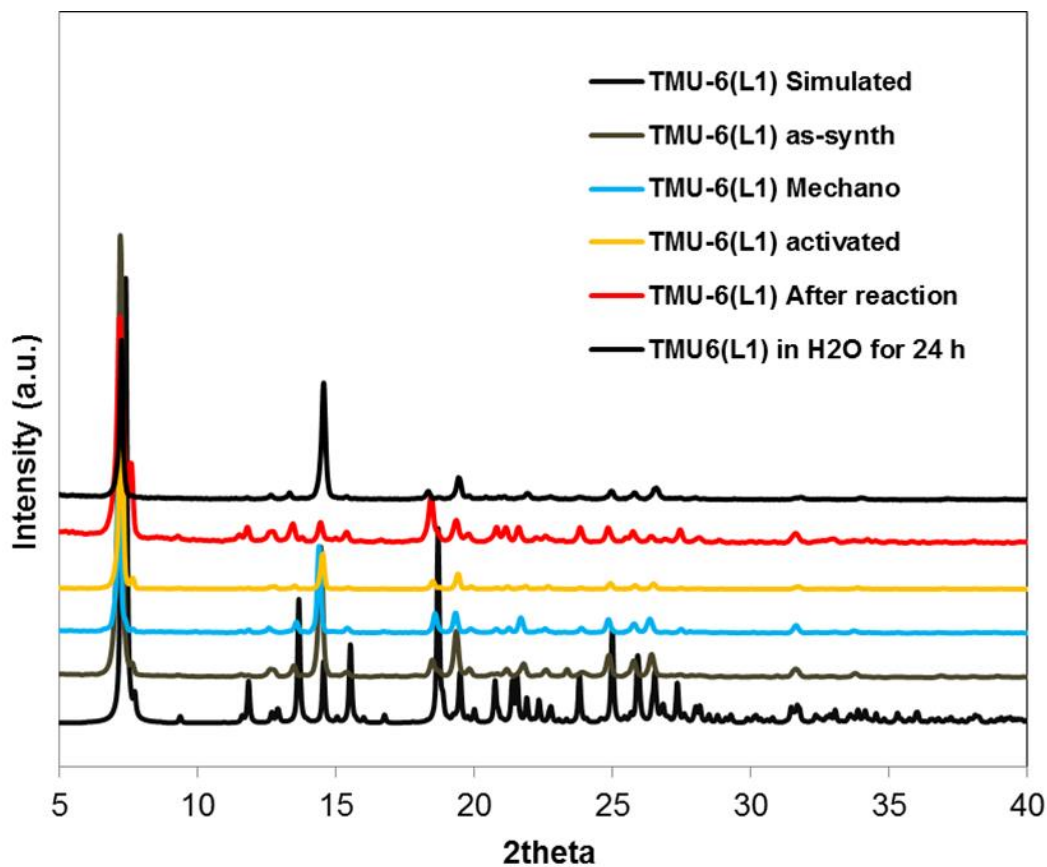


**Figure S13.** PXRD patterns of simulated, as-synthesized, mechano-synthesized, activated, after reaction and water stability of TMU-6(L1). The recycling PXRD of the MOFs were recorded after 7<sup>th</sup> cycle of reusability test.



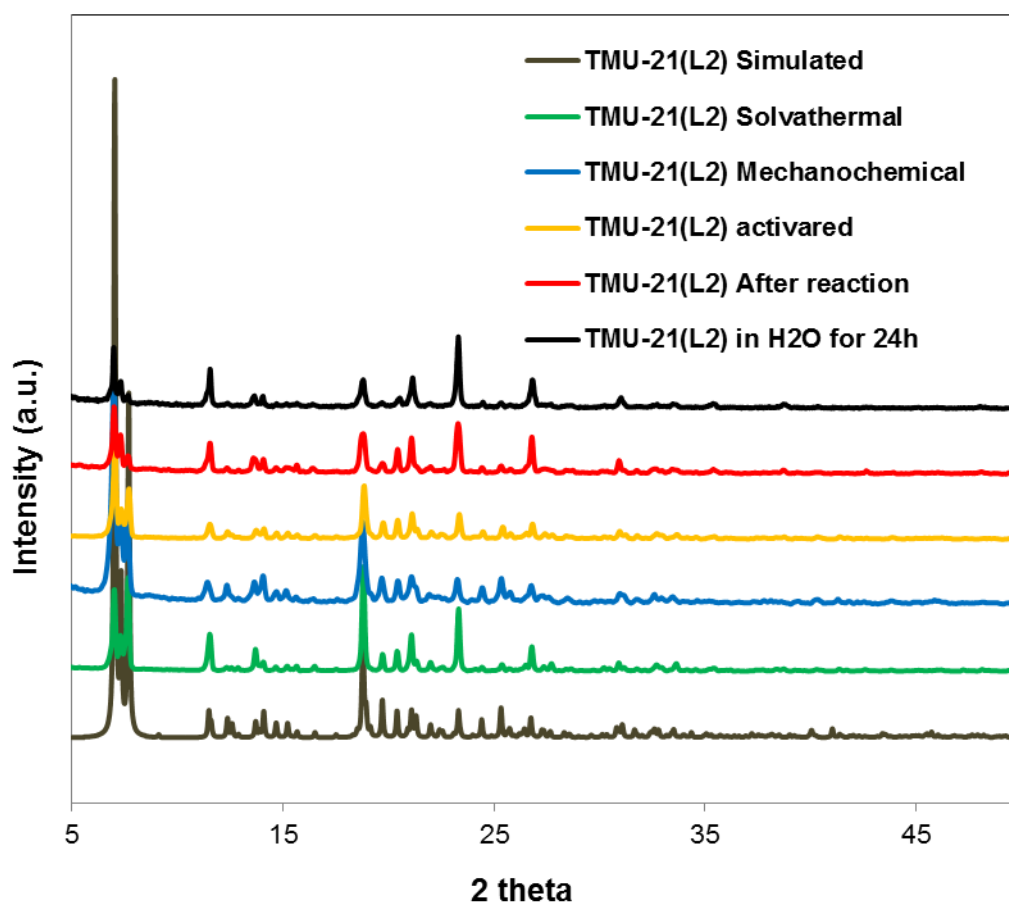


**Figure S14.** PXRD patterns of simulated, as-synthesized, mechano-synthesized, activated, after reaction and water stability of TMU-21(L2). The recycling PXRD of the MOFs were recorded after 7<sup>th</sup> cycle of reusability test.

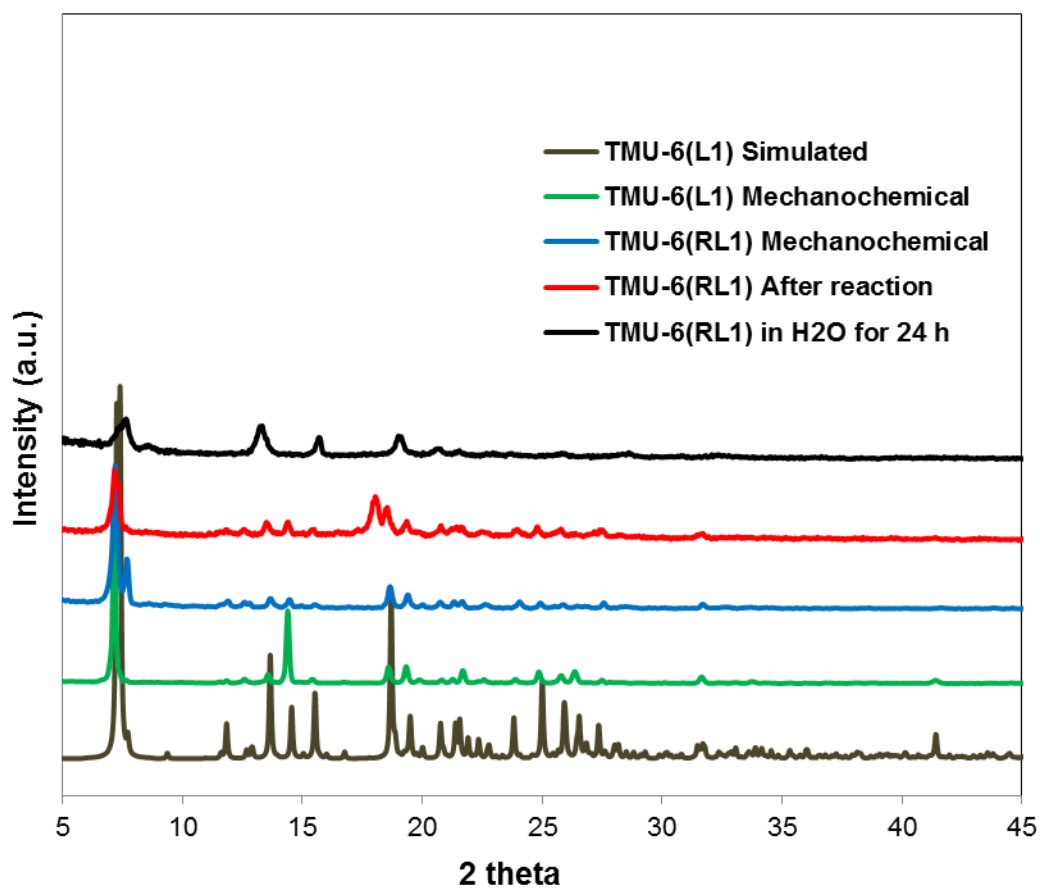


**Figure S15.** PXRD patterns of simulated, mechano-synthesized, after reaction and water stability of TMU-6(L1) and TMU-6(RL1). The recycling PXRD of the MOFs were recorded after 7<sup>th</sup> cycle of reusability test.

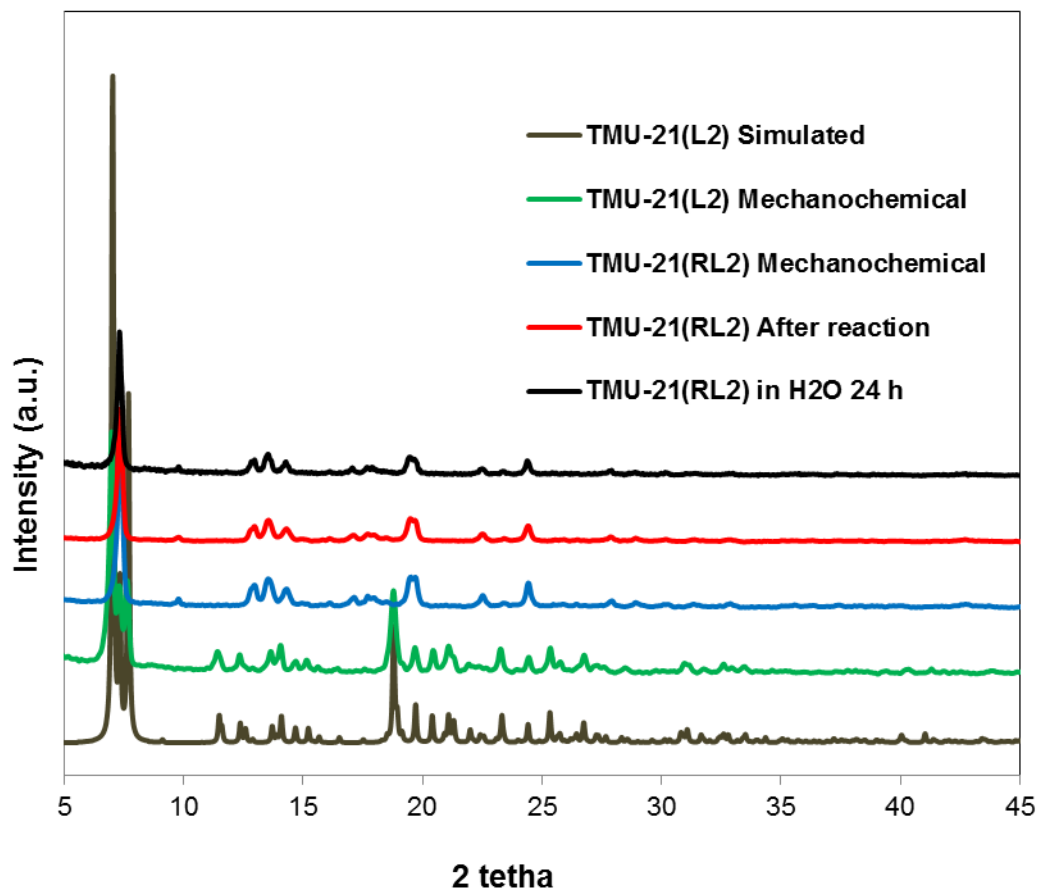


**Figure S16.** PXRD patterns of simulated, mechano-synthesized, after reaction and water stability of TMU-21(L2) and TMU-21(RL2). The recycling PXRD of the MOFs were recorded after 7<sup>th</sup> cycle of reusability test.

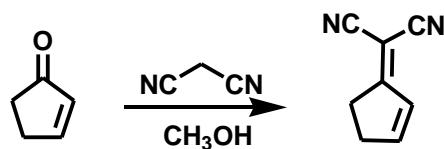
Time	TMU-21(L2)	TMU-6(L1)	TMU-6(RL1)	TMU-21(RL2)	control
MeOH R.T.	30	16.5	11	7.6	0.0
MeOH 60°C	60.5	45	40	36	0.0
EtOH 60°C	19.4	13	13.2	10	0.0

**Table S1.** Catalytic performance of TMU-6(L1), TMU-6(RL1), TMU-21(L2) and TMU-21(RL2), obtained by mechanochemical synthesis, within aldol condensation of malonitrile with 2-cyclohexen-1-one, 24h.

**Identification of the product:** 2-(cyclohex-2-enylidene)malononitrile

FT-IR data (KBr pellet,  $\nu/\text{cm}^{-1}$ ): 436(m), 570(m), 806(w), 1024(m), 1095(m), 1260(w), 1443(w), 1637(s), 2203(s), 2925(s), 3432(m)

$^1\text{H}$  NMR (500 MHz,  $\text{CDCl}_3$ ): 1.86 (m, 2H), 2.44 (m, 2H), 2.55 (t, 2H), 6.13 (m, 1H), 6.70 (d, 1H)



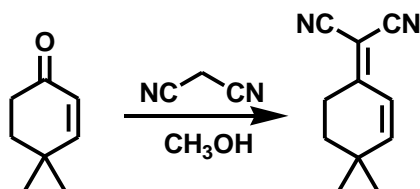
Time	TMU-6(RL1)	TMU-6(L1)	TMU-21(L2)	TMU-21(RL2)
12 h	54	47.8	40.2	25
24 h	93.7	89	76.3	60
36 h	97.3	99.2	93	80
60 h	---	---	99.5	95.4

**Table S2.** Time in depended catalytic performance of TMU-6(L1), TMU-6(RL1), TMU-21(L2) and TMU-21(RL2), obtained by mechanochemical synthesis within aldol condensation of malonitrile with 2-cyclopenten-1-one.

**Identification of the product:** 2-(cyclopent-2-enylidene)malonitrile

FT-IR data (KBr pellet,  $\text{v}/\text{cm}^{-1}$ ): 566(m), 1097(m), 1304(m), 1439(m), 1577(s), 1642(vs), 2204(vs), 2948(m), 3234(m), 3350(m)

$^1\text{H}$  NMR (500 MHz,  $\text{CDCl}_3$ ): 1.61 (m, 2H), 2.06 (t, 2H), 5.09 (m, 1H), 5.82 (d, 1H)



Time	TMU-21(L2)	TMU-6(L1)	TMU-6(RL1)	TMU-21(RL2)
12 h	53.5	42.8	38.5	27.6
24 h	72.7	53.4	48	31.3
36 h	87	72.4	69	63
60 h	91.4	80.8	77.8	70.3

**Table S3.** Time in depended catalytic performance of TMU-6(L1), TMU-6(RL1), TMU-21(L2) and TMU-21(RL2), obtained by mechanochemical synthesis, within aldol condensation of malonitrile with 4,4-dimethylcyclohexen-1-one.

**Identification of the product:** 2-(4,4-dimethylcyclohex-2-enylidene)malonitrile

FT-IR data (KBr pellet,  $\text{v}/\text{cm}^{-1}$ ): 682(m), 1022(m), 1219(m), 1456(m), 1553(m), 1605(s), 2192(s), 2959(m), 3209(m), 3347(m)

$^1\text{H}$  NMR (500 MHz,  $\text{CDCl}_3$ ): 1.14 (s, 6H), 1.71 (t, 2H), 2.83 (t, 2H), 6.45 (d, 1H), 6.62 (d, 1H)

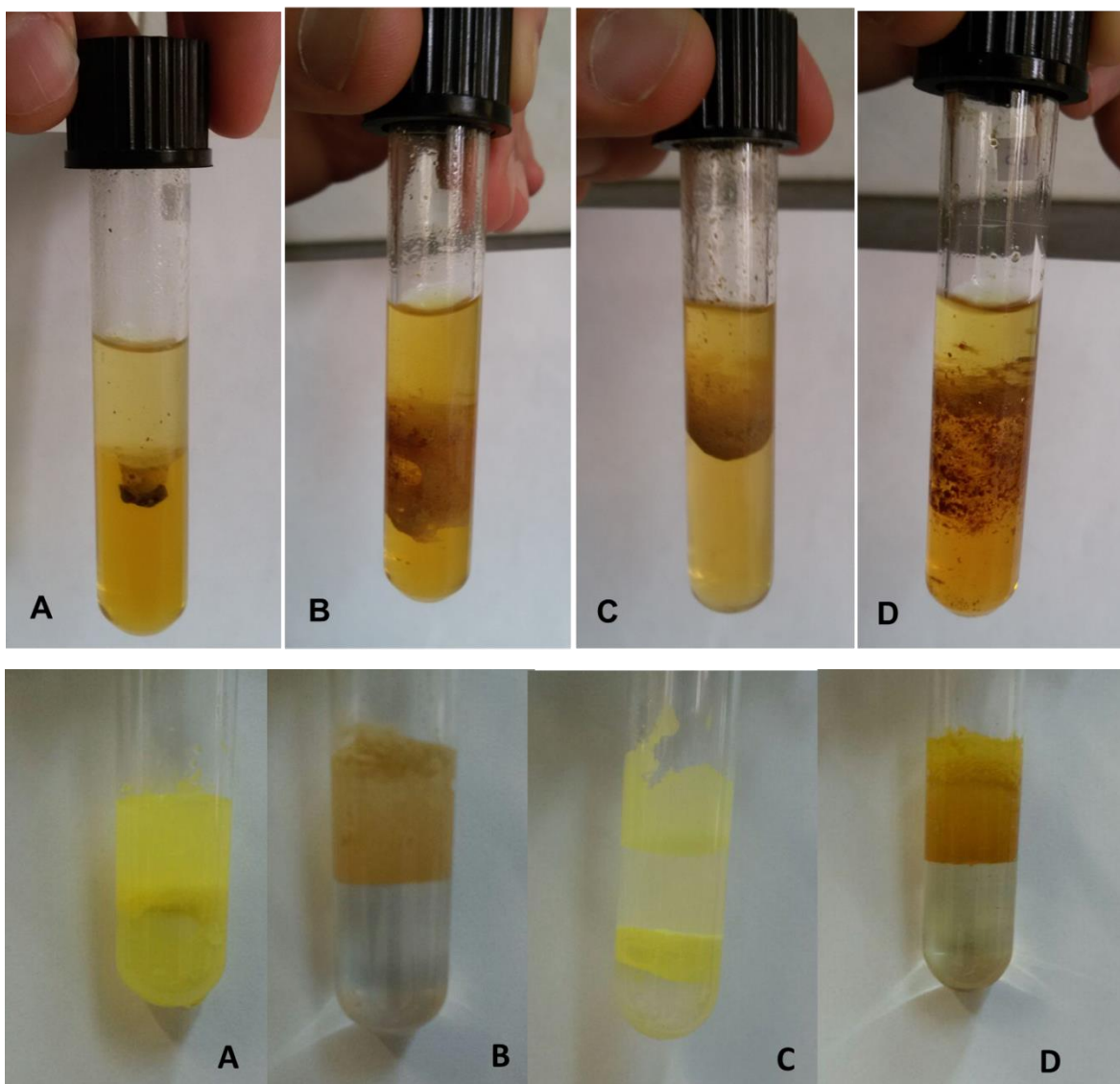


**Figure S17.** The images of the catalysts in H<sub>2</sub>O solvents after addition of toluene (up), in H<sub>2</sub>O solvents after addition of dichloromethane (down) (a) TMU-21(L2), (b) TMU-21(RL2), (c) TMU-6(L1) and (d) TMU-6(RL1).

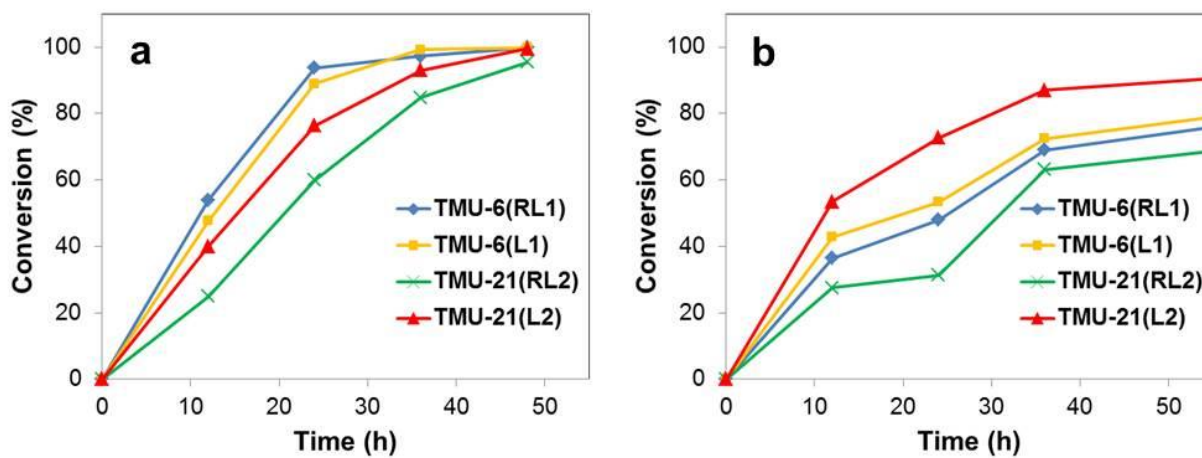


**Figure S18.** Yield-versus-time profile of aldol-type condensation reaction of (a) 2-cyclopenten-1-one and (b) 4,4-dimethyl-2-cyclohexen-1-one catalyzed by four MOF structures in the reaction conditions indicated in Table 1 of the manuscript.



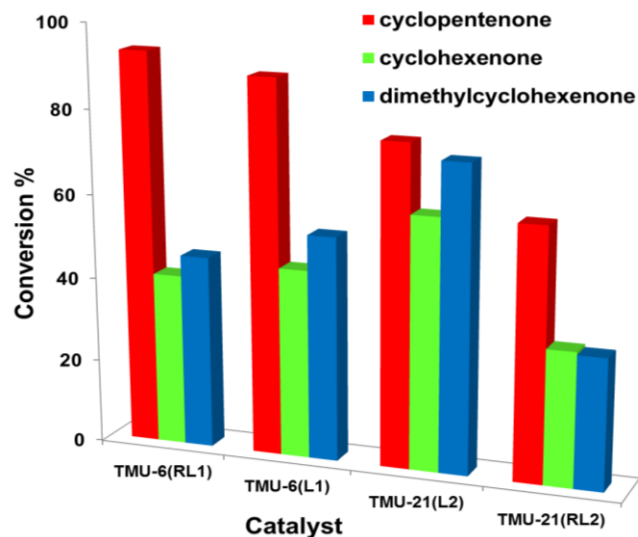


**Figure S19** Comparison of the catalyst reactivity of various substrates in the presence of different basic MOFs.

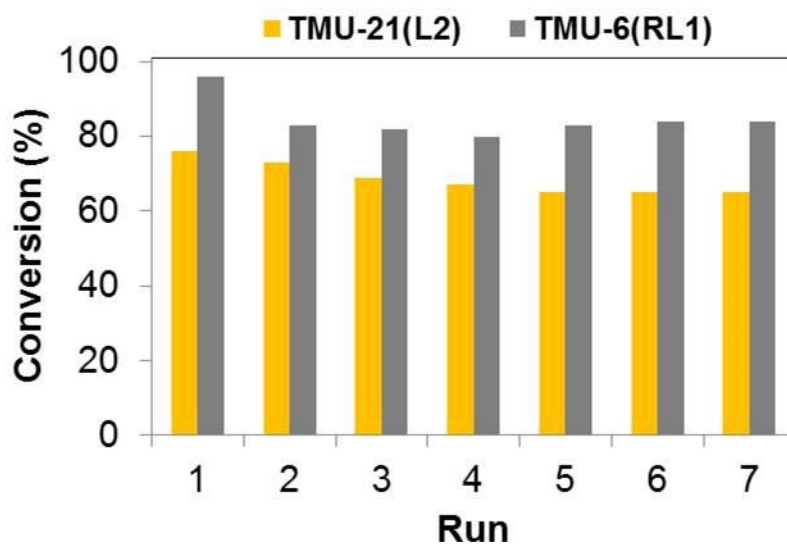


**Figure S20.** Reusability of TMU-6(RL1) (gray) and TMU-21(L2) (orange) in aldol-type condensation reaction of 2-cyclopenten-1-one and 4,4-dimethyl-2-cyclohexen-1-one (0.6 mmol), respectively. (Conditions: catalyst (5 mol%), malononitrile (0.9 mmol), MeOH, 60 °C, 24h)